Leakage-Induced Pipeline Stressing and its Potential Detection by Distributed Fiber Optic Sensing

A. Klar[1], R. Linker[2] and S. Herrmann[3]
[1]*Department of Civil Engineering, Technical University of Denmark, Lyngby, Denmark*
[1,2,3]*Faculty of Civil and Environmental Engineering, Technion – Israel Institute of Technology, Haifa, Israel*
E-mail: askla@byg.dtu.dk

ABSTRACT: The paper aims to develop an approximated analytical solution to model the bending moment profile in a sewage pipe, buried within an unsaturated soil, which occurs as a result of a leak. The solution involves evaluation of the greenfield displacements due to a buried point source, and its use as an input to a soil-pipeline interaction problem. The solution is extended for a general wetted sphere (having different degree of saturation with the radial distance). The final model is tested against finite element simulations of the coupled problem without the simplified assumptions and approximations, and is found to be satisfactory. The work may be considered a first step towards realization of a distributed fiber optic sensing system that, together with an appropriate spatial signal analysis, could identify leaks at their early stage. The current analysis indicates that the developed strain signal (and its profile) could be detectable for leaks having liquid loss as little as 300 to 500 liters.

KEYWORDS: Pipelines, Leaks, Soil-pipe interaction, Elastic solution, Sewage

1. INTRODUCTION

Leaks from sewage pipelines often go undetected for long periods of time, causing harm to both the environment and the health of the nearby population. This paper aims to advance a quick and efficient method of detecting such leaks before they cause dangerously high levels of contamination in their surroundings. Though a number of solutions exist for detecting other types of leaks, such as clean water or oil, given the unique nature of sewage pipelines few suitable methods exist for such systems. Unlike other substances, such as oils and gases, wastewater leak does not cause any noticeable change in temperature of the surroundings, rendering any technique relying on temperature irrelevant. Water pipelines are often monitored using pressure analysis, since a change in total pressure within a system of water pipelines indicates a potential leakage within the system. Sewage pipelines, however, tend to be designed using gravitational flow. A new method, considering the specific nature of sewage pipes, must be found in order to create an effective solution.

This paper focuses on the potential use of distributed fiber optic sensing as a tool for detecting leaks based on changes in the strain profile of the pipe. Unlike many existing techniques, which rely on a series of point-wise detectors, fiber optic cables can be used to measure tens of kilometers in a distributed manner, giving measurements every few centimeters. This provides a strain/deformation profile over the length of the entire pipeline, allowing for faster and more reliable results. It also eliminates the need for additional pinpointing method since both the existence and the location of the leak would be determined in the same step. Distributed fiber optic sensing has been suggested as a mean to detect tunnels and sinkholes through advance analysis of the spatial distribution of strain (e.g., Klar and Linker, 2010; Linker and Klar, 2017). It is suggested here that a similar approach could be applied to strain distribution along pipes for early detection of leaks.

The work detailed in this paper involves the development of an approximated analytical solution to describe the soil-pipe interaction and the bending moment which develops in the pipe, buried within an unsaturated soil, as a result of a leak. The solution uses the volume of liquid released due to a leak and the soil properties to determine the resulting stresses and strains. Such a model will provide the basis for developing an automated leak-detection system that uses fiber-optic-based strain measurements (which is not described in this paper).

The paper is composed of four main sections. Firstly, an analytical solution to the leak-induced ground deformation is developed. Secondly, this solution is introduced as an input to a soil-pipeline linear interaction problem to result in a normalized, general, solution for the problem. The solution and assumptions are then evaluated against a finite-element simulation of the coupled problem. Finally, the potential use of distributed fiber optic sensing for detecting such stains and detecting leakage from gravity pipelines is discussed.

2. FORMULATION

In order to develop an analytical solution to the problem at hand, a number of assumptions must be made about the pipeline response and about the leakage and its flow pattern through the surrounding soil. The following five assumptions are made: [1] The processes by which fluid flow and soil deformation occur may be considered as semi-coupled. In other words, there are two different sets of equations which are used, but only one set affects the other. In the present case, the independent set describes the flow through unsaturated soil and the dependent set describes the behavior of soil under stress changes. The flow causes swelling in the soil, which leads to deformations in the soil matrix; the suction, however, is not affected by those deformations once they have occurred. It should be noted that such an approximation may be considered appropriate only in the case of unsaturated soil where the flow is suction driven. In case of saturated soil, both the soil and the pipeline stiffness would affect the flow regime and hence the process cannot be decoupled. [2] The leakage is purely suction-driven, rather than gravitationally, and originates from an equivalent point source in the ground. This assumption is appropriate for clayey soils, in which suction plays a strong role in the flow, rather than for sandy soils, which do not develop strong suctions and will most likely be affected by gravity. [3] The decrease in suction due to wetting leads to a decrease in mean effective stress, which induces heave deformation based on the theory of linear elasticity in a semi-infinite half-space. [4] The pipeline, located within a continuum elastic domain (or a half-space of soil), is continuous and follows the Euler-Bernoulli beam theory, and its response to the heave deformation can be evaluated through linear elastic soil-pipeline deformation analysis. Finally, [5] an approximation is considered for describing the change in soil saturation, or wetness, as a function of distance from the source. Two different models are suggested in the paper: one follows the Green and Ampt (1911) approximation of a sharp wetting front, and the second consists of a steady state approximation developed in the paper.

2.1 Greenfield displacement due to spherical wetting

This section describes the solution for the greenfield displacement that occurs due to a spherical wetting. The term greenfield is used to describe a free soil response without the existence of the pipeline.

A leak which occurs below the surface can be treated as a buried spherical source in a semi-infinite domain, or a half-space.

Let us consider an effective stress linear elastic constitutive model, such that:

$$\sigma'_{ij} = K\epsilon_{kk}\delta_{ij} + 2GE_{ij} \tag{1}$$

where σ'_{ij} is the effective stress tensor, ϵ_{ij} is the strain tensor, and E_{ij} is the deviatoric strain tensor. δ_{ij} is the Kronecker delta. K and G are the bulk and shear moduli of the soil. It is assumed that the deformation of the soil is governed only by the effective stresses (which can alter due to changes in pore pressures or suction). The relation between the total stress, pore pressures, and the effective stress may be defined, in a simplified manner, using the averaged air and water pressures such that:

$$\sigma'_{ij} = \sigma_{ij} - \overbrace{\left(S_w p_w + S_g P_g\right)}^{\bar{p}} \delta_{ij} \tag{2}$$

where σ_{ij} is the total stress tensor, S_w is the water saturation, S_g is the gas saturation, p_w is the water pressure, and P_g is the gas (or air) pressure. Clearly this is a simplified model for unsaturated soil, and is equivalent to Bishop (1959)'s model with $\chi = S_w$. $\bar{p}$ is the equivalent pressure. Assuming the soil is exposed to the atmosphere, and $p_g = 0$, $\Delta\bar{p} = \gamma_w \Delta(S_w H_p)$, where H_p is the pressure head.

It can be shown (with details provided in Herrmann, 2017) that inside an infinite domain a change in the equivalent pressure, $\Delta\bar{p}$, will cause a change in the total stress of:

$$\Delta\sigma_m = \frac{4G}{3K + 4G}\Delta\bar{p} \tag{3}$$

where $\Delta\sigma_m$ is the mean total stress.

One may use the above expression for an infinitesimal volume in an infinite domain, and also obtain the displacement that develops around this volume. The expressions can then be used to establish the vertical displacement of the soil at the level of a wetted sphere (i.e. depth z_p Figure 1) by integration and superposition of mirror images and "relaxation of the free surface" by corresponding superposition of Boussinesq solution. The process is similar to that of Verruijt and Booker (1996) for tunnels, only that it is performed on a different deformation field derived from the wetted sphere.

The derived solution, representing the vertical displacement at leakage level (z_p) is:

$$u_{gf} = -\frac{R_f^3}{3K + 4G}\Delta\bar{p}\left(\frac{2z_p}{\left(x^2 + 4z_p^2\right)^{\frac{3}{2}}} + \frac{2A}{\pi}\right)$$

$$A = \int_0^{\pi} \frac{r\left(r^2 - 2z_p^2\right)}{\left(r^2 + z_p^2\right)^{\frac{5}{2}}\sqrt{(r+x)^2 + z_p^2}}\left[4(1 - \nu)K\left(\frac{4rx}{(r+x)^2 + z_p^2}\right) + \frac{2z_p^2}{(r-x)^2 + z_p^2}E\left(\frac{4rx}{(r+x)^2 + z_p^2}\right)\right] \tag{4}$$

where $K(\cdot)$ and $E(\cdot)$ are elliptic integrals of the first and second kind, respectively. ν is Poisson's ratio. R_f is the radius of the wetted sphere with equivalent pressure change of $\Delta\bar{p}$ (an estimation of which is provided in the following subsection). The equation above gives the displacement in the vertical direction occuring along the line of the source, at a horizontal distance *x* from the source.

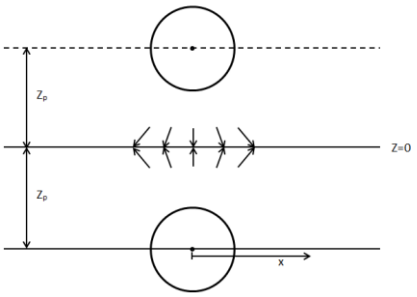

Figure 1 Superposition of mirror images and surface "relaxation" for obtaining a solution of half-space

2.2 Evaluation of term $R_f^3\Delta\bar{p}$

The term $R_f^3\Delta\bar{p}$ appears in Eq. 4, and constitutes the decoupled input. This paper examines two models. The first is based on the Green and Ampt (1911) approximation of the flow, which assumes that the wetted sphere around the source can be treated as a fully saturated compact sphere, with a sharp wetting front. The volume of this sphere can be calculated based on the amount of liquid which has been released. Since the entire void is filled with water, the wetted volume will be the volume of water in the sphere divided by the porosity, *n*, which by definition is equal to the saturated wetness, θ_s. The total volume of water in the sphere will be a combination of the initial wetness, θ_i, and the liquid loss, L_L. The radius of this sphere can then be calculated as:

$$R_f = \sqrt[3]{\frac{3}{4\pi}\frac{L_L}{\theta_s - \theta_i}} \tag{5}$$

In this case there are two distinct areas of interest - the wetted area, in which $S_w = 1$, and the non-wetted area, in which $S_w = S_i$ (the initial saturation degree). This means that the difference in pressure, $\Delta\bar{p}$, taken to be the difference in pressures between the inside of the wetted sphere and the outside. In other words, $\Delta\bar{p} = \bar{p}_{dry} - \bar{p}_{wet}$. Since the pressure head is equal to zero at full saturation, $\bar{p}_{wet} = 0$, the final term is:

$$R_f^3\Delta\bar{p} = \frac{3}{4\pi}\frac{L_L}{\theta_s - \theta_i}H_{pi}\gamma_w S_{wi} \tag{6}$$

where H_{pi} and S_{wi} are the initial head and saturation.

The second suggested method for calculating $R_f^3\Delta\bar{p}$ is based on a steady-state approximation, in which the total volumetric flow is considered to be a constant for any given time. This approximation can be used to find an analytical solution for the relationship between R_f, the radial distance from the source, and S_w at any given point. Since the saturation can be used to find the suction, this relationship can be used to determine the value of the equivalent pressure at a given R_f. The wetted region can then be broken down into spheres of increasing size - each with a lower saturation level - and those spheres can be superimposed onto one another to create an equivalent wetted sphere with a weighted equivalent pressure (simply because the soil responds linearly to the change of suction in the current model). In other words, $R_f^3\Delta\bar{p}$ can be calculated assuming first a very small sphere which is fully saturated, and then again for a slightly larger sphere with a slightly lower saturation level, and again until the saturation level of the final sphere is equal to the initial saturation

level in the soil, indicating that the edge of the wetted region has been reached. Mathematically, this can be described as an integral:

$$R_f^3 \Delta\bar{p} = \int_{\bar{p}_{initial}}^{\bar{p}_{final}} R_f^3(\bar{p}) d\bar{p} \tag{7}$$

To solve the above term, an equation must be derived which describes the relationship between R_f^3 and $\bar{p}$. This may be achieved by assuming that at any given point in time (i.e. radial distance from the source), the volumetric flow, Q, can be considered a constant:

$$Q = 4\pi r^2 k_s k_r(S_w) \cdot \frac{\partial H_p}{\partial S_w} \cdot \frac{\partial S_w}{\partial r} = C \tag{8}$$

where k_s is the saturated hydraulic conductivity of the soil and k_r is its relative permeability (function of degree of saturation). Eq. 8 can be used to form a numerical relation between the radius and the degree of saturation such that:

$$\Delta r = \frac{4\pi r^2 k_s k_r(S_w)}{C} \cdot \frac{\partial H_p}{\partial S_w} \cdot \Delta S_w \tag{9}$$

The liquid loss on the other hand is equal to:

$$L_L = \int_{r_0}^{\infty} 4\pi r^2 n dS_w(r) dr \tag{10}$$

One can iterate on the constant C to achieve the $S_w(r)$ profile for a given liquid loss. Note that once $S_w(r)$ is solved, so is $R_f^3(\bar{p})$ and Eq. 7 (which provides the desired value).

2.3 The response of the pipeline to the leakage

The response of the pipeline to the leakage may be solved by introducing the greenfield displacement into the elastic continuum solution of Klar (2005) which uses a matrix formulation. It can also be solved through Fourier transform as suggested by Klar (2017) and Klar (2018), answering also cross-sectional compatibility, but this is beyond the scope of this paper.

The matrix-based formulation answers the following set of linear equations:

$$\left[[S] + [K^*] + [K^*][\lambda_s^*][S]\right]\{u\} = [K^*]\{u_{gf}\} \tag{11}$$

where $[S]$ is the stiffness matrix of the pipeline, $[K^*]$ is the local stiffness matrix of the soil, representing the soil resistance to local loads, $[\lambda_s^*]$ is the interaction matrix, representing the soil displacement at various locations to loads at other locations, $\{u\}$ is the pipeline displacement and $\{u_{gf}\}$ is the greenfield soil displacement, defined earlier in Eq. 4 for the current problem. Solving for $\{u\}$ results in the final deformation of the pipeline due to the leak-induced swelling.

2.3.1 Maximum bending moment along the pipe

It is convenient to normalize the pipeline bending moment by that of the greenfield. That is, by that obtained through forcing the pipeline to follow the greenfield condition, $M_{gf}(x) = -EId^2u_{gf}(x)/dx^2$ (EI being the flexural stiffness of the pipe). Introducing Eq. 4 to this term, and extracting the maximum value results in:

$$M_{max,gf} = EIR_f^3 \Delta\bar{p} \frac{3(7-4\nu)}{64Gz_p} \frac{4G}{4G+3K} \tag{12}$$

The above bending moment represents the maximal possible value in the pipe, as it does not include the pipeline resistance to the greenfield displacement. Bending moments based on the soil-pipe interaction solution (Eq. 11) will always be smaller. In fact $M_{max,gf}$ may be used to normalize the response. A curve fitted solution to multiple analyses performed with Eq. 11 resulted in:

$$M_{norm} = \frac{M_{max}}{M_{max,gf}} = \frac{1}{1+\frac{4}{5}R^{2/3}} \tag{13}$$

where R is the relative pipe-soil stiffness for the considered problem, defined as:

$$R = \frac{EI}{Gr_p^{1/2} z_p^{7/2}} \tag{14}$$

where r_p is the pipeline radius and z_p is its central depth.

When the pipeline is flexible (low EI value) or the soil is stiff (high G), R will tend to be of small values, and the normalized bending moment will tend to become unity. As R increases, the normalized bending moment decreases. Eq. 12 together with 13 and 14, can be used to establish the value of the expected maximum bending moment in the pipeline, M_{max}.

3. VERIFICATION AND EVALUATION

In order to evaluate the suggested models, a comparison to finite element simulations of the problem in COMSOL Multiphysics was considered. The COMSOL simulations considered also a semi-coupled problem in which Richards (1931) equations were first used to establish the wetting of the soil due to a point leakage from the pipeline, followed by the mechanical response of the pipeline. The COMSOL solution considers the boundary condition more accurately, in the sense that the leakage induced wetting is not assumed to be spherical but develops naturally as a function of the governing equations and boundary conditions. In the simulation the pipe was modeled as an empty concrete cylindrical tube (with wall thickness represented by 3D material elements rather than shell elements). Leak was induced by setting a boundary condition such that at a particular point along the edge of the pipe, the soil would be at full saturation throughout the simulation. This created a difference in the total head between that region and the rest of the soil, causing flow to occur from the region of higher head toward soil with a lower head. In order to keep the model consistent with the idea of gravitational rather than pressure-based flow, the pressure head representing the leak cannot be greater than the radius of the pipeline; any greater pressure head would mean that there would have to be pressure within the pipe, and would not be an accurate representation of the type of sewage pipelines considered in this work. Figures 2 and 3 show the COMSOL model, which consists of a concrete pipeline with an external radius of 27 cm and internal radius of 22 cm at the depth of 4 m, and the small hole at the side of the pipeline constituting the source of leakage.

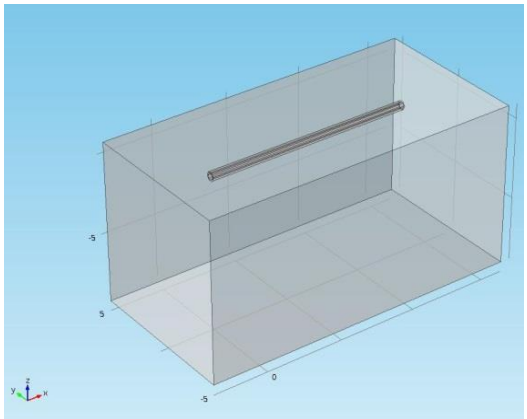

Figure 2 COMSOL model: buried pipe in soil cube

In all simulations and analytical calculations, the unsaturated soil characteristics answered the van Genuchten (1983) model for Beit Netofa Clay, and the initial head was set to minus 70 m.

Figures 4 to 6 illustrate the development of the "wetted sphere" (using contours of wetness), starting by being similar to a hemisphere, due to the existence of the pipeline itself, and later extending in radius, covering the entire pipeline. The sphere representation is no longer valid when the wetting front reaches the surface or the side boundary. In fact, it may be said that the suggested analytical model is only relevant to the intermediate condition in which the wetted area is sufficiently large to resemble a sphere surrounding the pipeline (as in the assumptions of the analytical solution), but does not reach the surface.

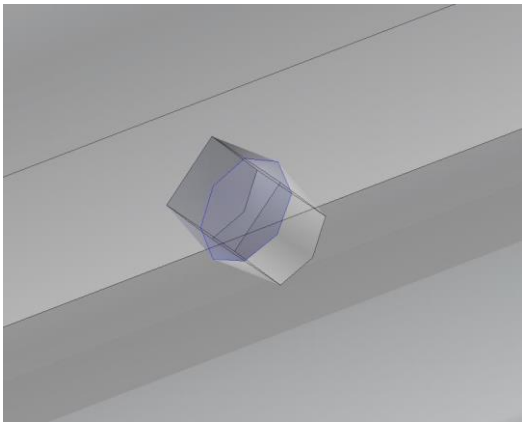

Figure 3 Pressured boundary along the edge of the pipe

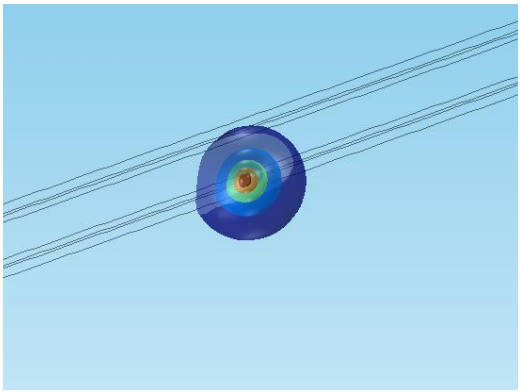

Figure 4 Wetter sphere around leak at early stages

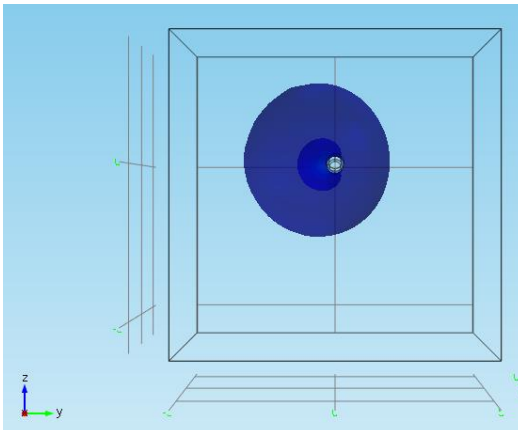

Figure 5 Wetted volume when liquid loss of 4.3m^3

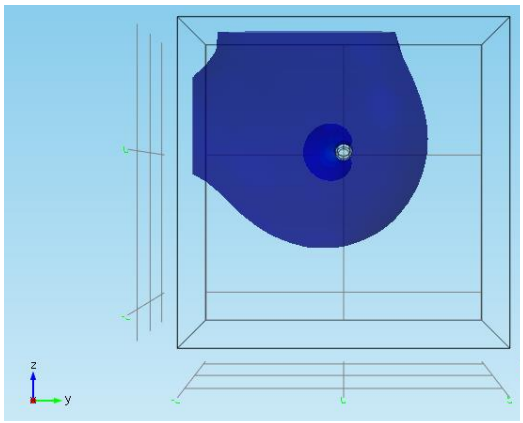

Figure 6 Wetted volume when liquid loss of 8.6m^3

Figure 7 shows a comparison between the COMSOL ground wetting solution to that based on the two simplified analytical models presented in section 2.2. It is clear from the comparison that, for this considered case, the steady state approximation provides a better prediction than the Green and Ampt based solution which involves a sharp wetting front. It is therefore expected that the pipeline response calculated using the steady state approximation will also be more similar to that of COMSOL.

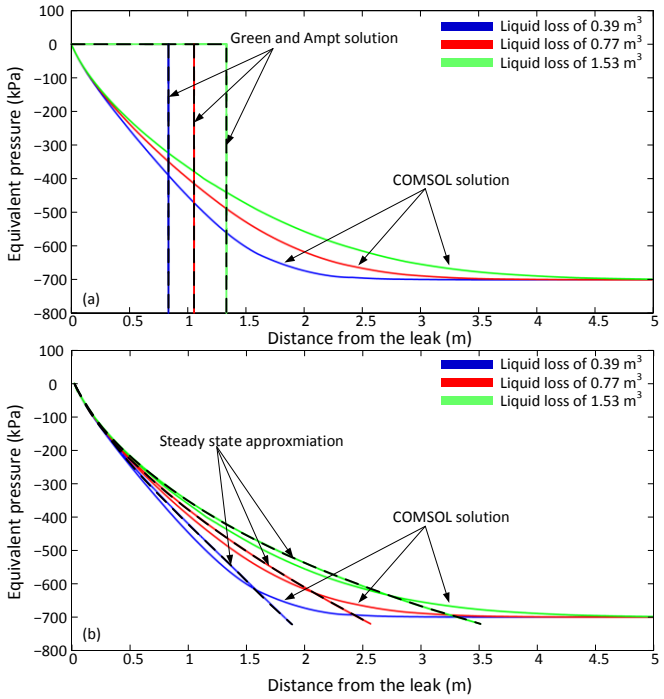

Figure 7 Equivalent pressure distribution based on the various models. Comparison between the COMSOL solution and (a) the Green and Ampt solution; (b) the steady state approximation

Figure 8 shows a comparison between the maximum bending moment obtained by the COMSOL complete analysis and that obtained by the use of Eqs. 12 to 14, both under the Green and Ampt flow solution and the steady state approximation. Note that for each liquid loss, multiple analyses were performed with the stiffness of the soil ranging from about 5 to 50 MPa (for Young's modulus). The solution based on Green and Ampt approximation underestimates the developed bending moment. The solution based on the steady state assumption, however, provides fair estimates for the maximum bending moments, with better prediction with increasing liquid loss.

This is expected considering the spherical model becomes more accurate as the leakage increases, up to the point where the wetting front reaches the surface.

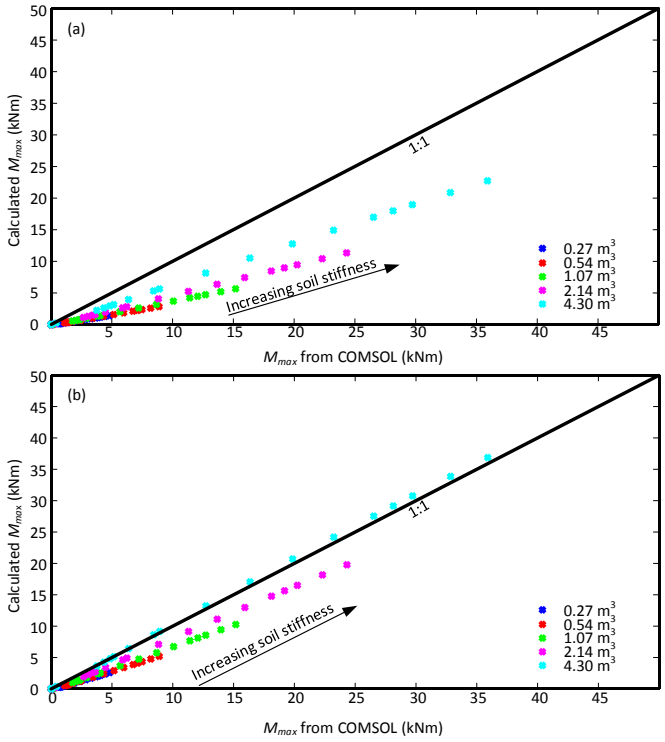

Figure 8 Comparison of maximum bending moment in the pile between the COMSOL simulation and the analytical solution based on (a) the Green and Ampt approximation, (b) the steady state approximation. The colors correspond to different amount of leakage as indicated in the Figures

Figure 9 shows a comparison of the bending moment distribution obtained from the COMSOL analysis to that based directly on the linear set of equations for the soil-pipeline interaction (Eq. 11) together with the input of greenfield displacement based on the steady state solution. The COMSOL bending moment distribution was obtained by assuming an Euler-Bernoulli response of the COMSOL pipeline and evaluating the bending moment based on the difference in strain values between the crown and the invert of the pipeline. While the solution does not match perfectly, the overall agreement is rather reasonable, considering the complexity of the problem and the simplicity of the suggested solution. As before the solution becomes more accurate with increasing liquid loss, since the "spherical wetting" assumption becomes more valid.

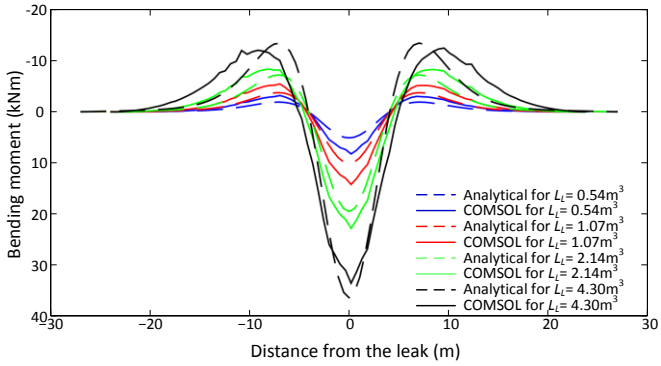

Figure 9 Comparison of bending moment distribution for various liquid losses assuming relative rigidity, *R*, of 0.3

4. DETECTABILITY OF STRAIN

For this method to be usable in a fiber-optic-based leak detection system, the levels of strain must be high enough to cause a detectable frequency shift (for example of backscattered Brillouin light). Current technologies of Brillouin sensing allow accuracy of a few microstrains. For evaluation of the expected strain levels, multiple analysis cases were considered in which both the pipeline stiffness and the soil varied within a reasonable range relevant for clay soils in arid zones (like Israel). For each of the leakage scenarios, the maximum strain value was evaluated. Since the analysis considered different pipe and soil parameters, a range of strain levels corresponding to each particular amount of liquid loss was established. Table 1 shows the expected maximum strains caused by different leakage amounts, as calculated analytically for the Beit Netofa Clay.

Based on the minimum value seen within each range, the amount of liquid loss that is expected to cause noticeable and measurable strain is around 270 to 540 liters, although this depends also on the soil and pipe parameters. These small values indicate that the approach could potentially be applied for detection of early leakage, at least in arid zones where the potential for leakage-induced heave is substantial.

Table 1 Expected strain levels in response to various leakage amounts

Liquid Loss (Liters)	Expected strain (με)
130	1.5-4
270	2-6
540	4-13
1070	7-25
2150	15-50
4300	25-90
8600	45-160

5. SUMMARY AND CONCLUSION

Leaks from sewage pipelines pose a threat to the environment as well as the health of the nearby population. The motivation behind the work presented in this paper is the need to assess damages in underground sewage pipelines accurately and effectively, allowing leaks to be detected before they cause high levels of contamination in the surrounding area. Since sewage pipes are typically designed with gravitational flow and the material inside them is not one which would incur significant temperature changes in the surrounding region when leaking, methods which rely on pressure or temperature sensing are not appropriate. It is suggested that distributed fiber-optic-based strain sensing, together with an appropriate algorithm for recognizing the leakage-induced strain changes, provide such early leak detection.

The research presented in this work demonstrates the successful development of a new analytical model to describe leakage-induced pipeline stressing. The solution relates the total volume of liquid loss from a leak to the resulting bending moment profile. This was derived by combining an equation for the greenfield displacement with one that considers the soil-pipe interaction. To finalize the solution, an approximation was needed to describe the change in saturation as a function of distance from the source. Of the two approximations examined, one was found to be more suitable to the particular problem at hand, and was used in the final calculations.

The overall solution was assessed through a series of coupled unsaturated flow and deformation finite element simulations, not involving the above approximations. From the comparison, the analytical solution was shown to be relatively accurate. The model developed is comprehensive, and can be used for various soil types or pipe parameters. It provides reasonable results, keeping in mind certain constraints (such as the shape of the wetted area and its extent).

This indicates its potential as a component of a fiber-optic-based detection system, in which data would be analyzed in real time to determine if and where a leak has occurred.

Clearly, further work is required for the development of such a system, both to better understand the soil structure interactions and to consider the flow regime that develops in the more realistic configuration of layered soil and pipelines buried within trenches. Further work should also be performed to include soil nonlinearity and stress dependency.

6. ACKNOWLEDGMENT

The work presented in this paper summarizes the MSc thesis of Shoshana Herrmann. The authors wish to thank the Technion Grand Water Research Institute for financially supporting this project and providing a scholarship for S. Herrmann.

7. REFERENCES

Bishop, A.W. (1959) "The Principle of Effective Stress", Teknisk Ukeblad 39 (October). Pp. 859–863.

Green, W. Heber; Ampt, G. A. (1911). "Studies on Soil Physics". The Journal of Agricultural Science.

Klar, A. (2017) "Exact elastic continuum solution for tunneling effects on buried pipelines", In Proc. of the IV International Conference on Computational Methods in Tunneling and Subsurface Engineering, EURO:TUN 2017 (pp. 423–430). Innsbruck.

Klar, A. (2018) "Elastic continuum solution for tunneling effects on buried pipelines using Fourier expansion", ASCE Journal of Geotechnical and Geoenvironmental Engineering. Under review.

Klar, A., and Linker, R. (2010) "Feasibility study of automated detection of tunnel excavation by Brillouin optical time domain reflectometry", Tunnelling and Underground Space Technology, 25(5), 575–586.

Klar, A., Vorster, T. E. B., Soga, K., and Mair, R. J. (2005) "Soil-pipe interaction due to tunnelling: comparison between Winkler and elastic continuum solutions", Geotechnique, 55(6), pp. 461–466.

Linker, R., and Klar, A. (2017) "Detection of Sinkhole Formation by Strain Profile Measurements Using BOTDR: Simulation Study", Journal of Engineering Mechanics, 143(3), B4015002.

Herrmann, S. (2017) "Leakage-Induced Pipeline Stressing", MSc dissertation, Technion – Israel Institute of Technology.

Richards, L.A. (1931). "Capillary conduction of liquids through porous mediums". Physics. 1 (5), pp. 318–333.

van Genuchten, M. T. (1980) "A Closed-form Equation for Predicting the Hydraulic Conductivity of Unsaturated Soils". Soil Science Society of America Journal, 44(5), pp 892-898.

Verruijt, A., and Booker, J. R. (1996) "Surface settlements due to deformation of a tunnel in an elastic half plane", Geotechnique, 46(4), pp. 753–756.